TÜBİTAK

Turkish Journal of Chemistry

http://journals.tubitak.gov.tr/chem/

Research Article

Turk J Chem
(2018) 42: 1136 – 1145
© TÜBİTAK
doi:10.3906/kim-1802-25

The design and synthesis of a photo-controlled, peptide-based potential drug carrier

Melek PARLAK KHALILY[1], **Salih ÖZÇUBUKÇU**[1,2,*]

[1]Department of Chemistry, Faculty of Arts and Science, Middle East Technical University, Ankara, Turkey
[2]Department of Biotechnology, Graduate School of Natural and Applied Sciences, Middle East Technical University, Ankara, Turkey

Received: 12.02.2018 • **Accepted/Published Online:** 06.05.2018 • **Final Version:** 03.08.2018

Abstract: Our focus in this study is on the design and synthesis of a light-responsive peptide-based nanocarrier in order to develop effective and biocompatible drug delivery systems. The synthesized nanocarrier is basically composed of peptide amphiphiles comprising a micelle forming a Pro-Pro-Pro-Lys-Lys-Lys peptide sequence with an attached anthracene fluorophore. Anthracene containing an inner core of the micelle can serve as a storage site for poorly water-soluble drugs. Moreover, anthracenes that come in close proximity with the formation of micellar structures can undergo photodimerization upon irradiation at 365 nm, which disrupts the micelle structures formed by the self-assembly of the peptide amphiphiles. Therefore, if a drug is encapsulated within the hydrophobic core of this peptidic carrier system, its release can be induced by the controlled exposure of the anthracene moiety to UV light.

Key words: Self-assembly, micellar peptides, photodimerization, anthracene

1. Introduction

The recent advances in stimuli responsive systems make on-demand drug delivery applicable in the field of nanomedicine. Because the delivery of a drug in spatial-, temporal-, and dosage-controlled fashions is clinically important, nanocarriers with structures that are transformable in response to external stimuli have gained increasing attention.[1] A broad range of nanocarriers with diverse sizes, architectures, and physiochemical properties have been designed. These include self-assembled peptide nanostructures, liposomes, polymer nanoparticles, dendrimers, and inorganic nanoparticles made of iron oxide, quantum dots and gold or metal oxide frameworks.[1,2]

Material scientists have designed or modified the existing nanocarriers to fulfill the requirements of ideal drug delivery systems, which are biocompatible, and have a large drug payload with a controlled release function.

On-demand drug delivery systems take advantage of stimuli signals that are basically categorized into two main types: internal stimuli and external stimuli. The intracellular environments of normal tissue and diseased tissue may differ in pH values, reduction–oxidation reaction (redox) states, and the types and amounts of biomolecules.[2] These natural gradients make internal stimuli ideal triggers for the controlled release, and thus enhance the specificity of carrier. On the other hand, external stimuli play an equally important role too. Exposure to temperature changes, magnetic fields, ultrasound waves, and light and electrical fields are examples of generally used external stimuli.[1,2]

*Correspondence: osalih@metu.edu.tr

Light-induced drug delivery remains among the most popular stimuli-responsive strategies owing to its noninvasive nature and the possibility of remote spatiotemporal control. The drug-releasing behavior of light-triggered systems can be precisely controlled by applying specific light irradiation at a specific position. Photodimerizations, *cis*−*trans* photoisomerization, photocleavage of chemical bonds, and photoinduced heating of gold nanoparticles (AuNPs) are some examples of light-induced mechanisms. Among these, photodimerization is one of the oldest and most well-established mechanisms for manipulating various types of light-sensitive molecules.[3] The photodimerization reaction can be reversed upon the application of an appropriate wavelength of light. This simple reversible reaction, which allows a rapid change in the size of molecules, has generated considerable interest in the development of new photoresponsive systems for diverse applications—in particular, drug delivery. The first example of a photoresponsive delivery system was based on the photodimerization reaction of coumarin, which was developed by Fujiwara et al. in 2003.[4,5] Coumarin undergoes a [2+2] photodimerization reaction, forming a cyclobutane dimer. This feature of coumarin-containing materials leads to effective and direct control over the guest uptake and release.

Apart from coumarin, anthracene and its derivatives have been used in many light-responsive systems.[6−20] Although anthracene shows some toxicity in the living systems, its derivatives are not necessarily toxic. This enables their use in drug delivery applications.[18−20] The photophysical and photochemical properties of the photodimerization reaction of anthracene, which occurs favorably under UV light irradiation (250–400 nm), have been widely investigated for the application of photo-responsive materials. Although dimerization has recently been accomplished with visible light (400–700 nm) or multiphoton light in order to decrease side effects during irradiation,[15−17] a typical dimerization reaction takes place upon irradiation at 365 nm at the ninth and tenth carbon atoms (Scheme 1). This photochemical transformation can be easily monitored by fluorescence spectroscopy, as the anthracene core responsible for the molecule's emission at 470 nm is disrupted upon dimerization, thus providing a trail for following the progress of the reaction. The photodimer is found to be thermally stable with no indication of dissociation at room temperature; however, dimerization may be reversed either by irradiation at 254 nm or by heating to more than 100 °C.

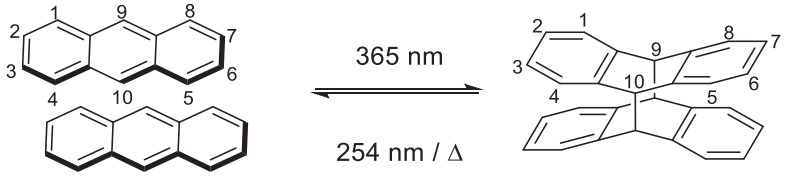

Scheme 1. The [4+4] cycloaddition reaction of anthracene and its reverse reaction.

In the present study, our main goal was to take advantage of the photoactive anthracene moiety to synthesize a light-activated drug delivery system. For this purpose, we designed and synthesized a novel anthracene-containing, micelle-forming peptide and investigated the structural disruption of peptide assembly with UV light.

2. Results and discussion

In order to incorporate anthracene into peptide structure, anthracene-2-carboxylic acid was synthesized by following a procedure described in the literature.[21] First, 2-methylanthraquinone (**1**) was oxidized to obtain anthraquinone-2-carboxylic acid (**2**) using chromium trioxide-acetic acid in high yield. Then anthraquinone-2-

carboxylic acid was reduced to anthracene-2-carboxylic acid (**3**) by means of zinc–ammonia and the expected product was isolated in 72% yield as a crystalline compound (Scheme 2).

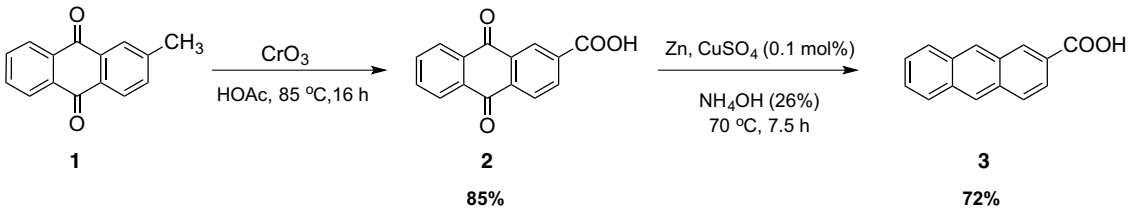

Scheme 2. Synthesis of anthracene-2-carboxylic acid (**3**).

Peptide amphiphiles typically consist of a hydrophilic, a peptide head group, and a hydrophobic alkyl tail. Micelle-forming Pro-Pro-Pro-Lys-Lys-Lys peptide[22] was chosen as the head group and it was synthesized by using solid-phase peptide synthesis (SPPS) following Fmoc strategy on Rink amide resin. 6-Aminohexanoic acid (Ahx) was used both as an alkyl tail and a spacer to increase the conformational freedom of the anthracene moiety. Anthracene-2-carboxylic acid (**3**) was coupled to Ahx-Pro-Pro-Pro-Lys-Lys-Lys peptide while peptides were still on resin. Then it was cleaved from resin via TFA, resulting in an anthracene-Ahx-Pro-Pro-Pro-Lys-Lys-Lys (Ant-PK) peptide (Figure 1).

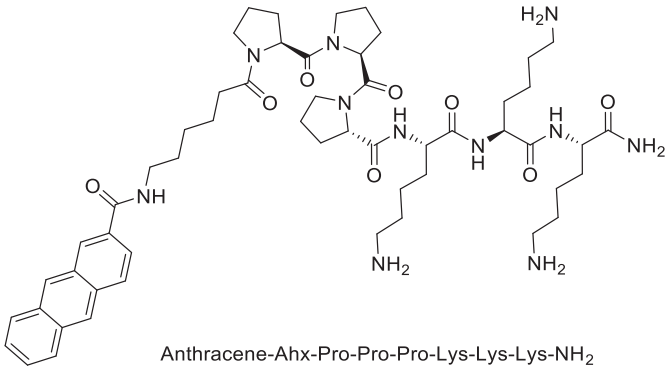

Figure 1. Chemical structure of Ant-PK.

After the synthesis of Ant-PK, it was purified by reverse phase high performance liquid chromatography (RP-HPLC) using a C18 column. In order to obtain peptide micelles, 0.5 wt. % Ant-PK peptide solution was prepared in water and the pH of the peptide solution was set to 11 using 1 M NaOH solution to neutralize positive charges on lysine residues. However, contrary to our expectations, both transmission electron microscopy (TEM) images and dynamic light scattering (DLS) analysis indicated no evidence of micellar structure. In light of this finding, the pH of the peptide solution was fixed to 4 using 1 M HCl solution. TEM images proved that peptides were self-assembled into micelles around 100–200 nm in size, even though lysine residues were positively charged under acidic pH (Figure 2).

Hydrodynamic size of peptidic micelles was also analyzed by DLS measurement and the mean of ten measurements was taken. Average hydrodynamic size was 468 $\pm$ 74 nm, as shown in Figure 3. Since it is known that charged peptides are quite hydrophilic, the thickness of the hydration layer was reasonable and consistent with the particle size obtained from the TEM image.

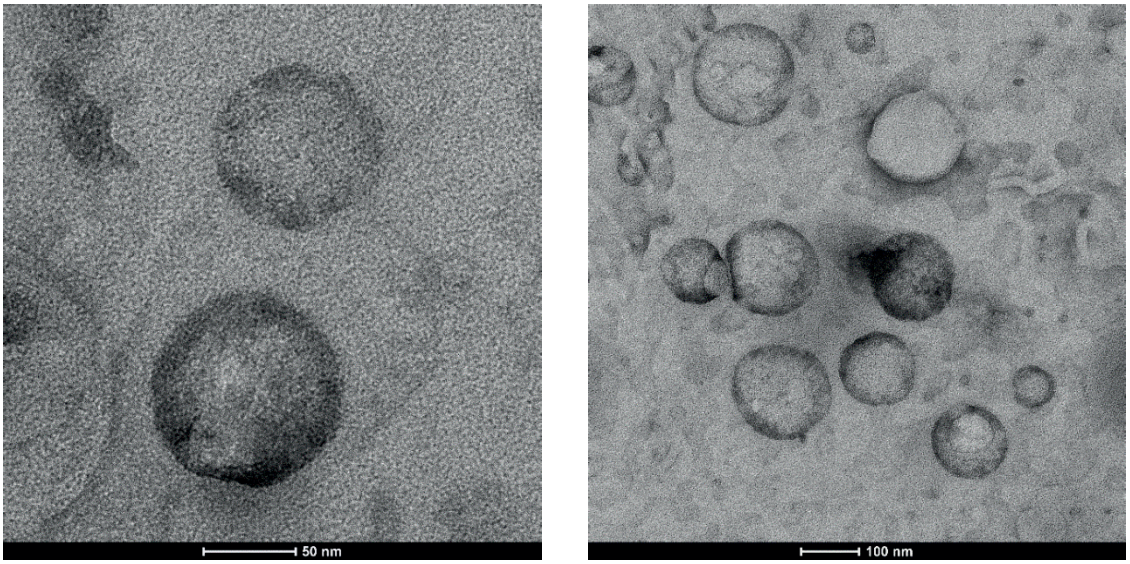

Figure 2. Positively stained TEM image of Ant-PK peptide at pH 4.

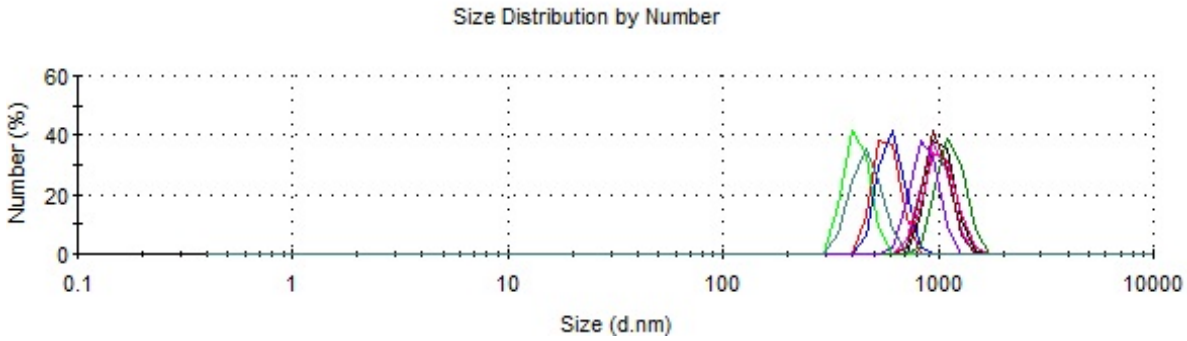

Figure 3. Particle size distribution graph of Ant-PK peptide before irradiation.

Irradiation experiments were performed with aliquots taken from the peptide solution in 10-min irradiation intervals with a total irradiation time of 30 min. Because the extended Π-systems in anthracene were broken via dimerization reaction, fluorescence emission that drives from fully conjugated aromatic system was decreased significantly. Therefore, dimerization was followed with anthracene emission spectra in an aqueous solution. The intensity of the maximum emission peak at 440 nm was decreased by irradiation. On the basis of the signal intensity decrement, overall conversion of the photodimerization reaction was 59% (Figure 4).

The TEM image of peptide after 30 min of irradiation indicated the partial disruption of micellar structure because of the conformational changes in anthracene structure (Figure 5A). DLS measurements also supported this structural change. Average hydrodynamic size was 993 ± 165 nm, as shown in Figure 5B. In consideration of these findings, the designed peptidic photoresponsive micellar system can be used a potential drug carrier.

To summarize, we synthesized a peptide-based potential nanocarrier with photoactive anthracene moiety. An aqueous solution of Ant-PK peptide formed a micellar structure at pH 4. Irradiation of the peptide system with a 365 nm light source partially disrupted their structure, thus providing control over their structural integrity. Despite the fact that some hurdles remain to be overcome, the results presented in this study demonstrate that these systems are very promising for controlled drug release with noninvasive light exposure.

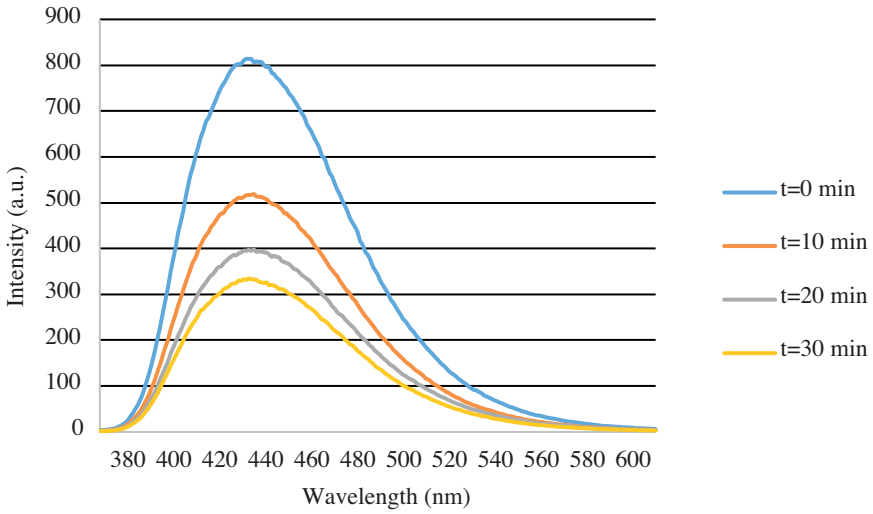

Figure 4. Fluorescence emission intensity of Ant-PK at 125 μM (0.5 wt. %) with λ_{ex} = 365 nm.

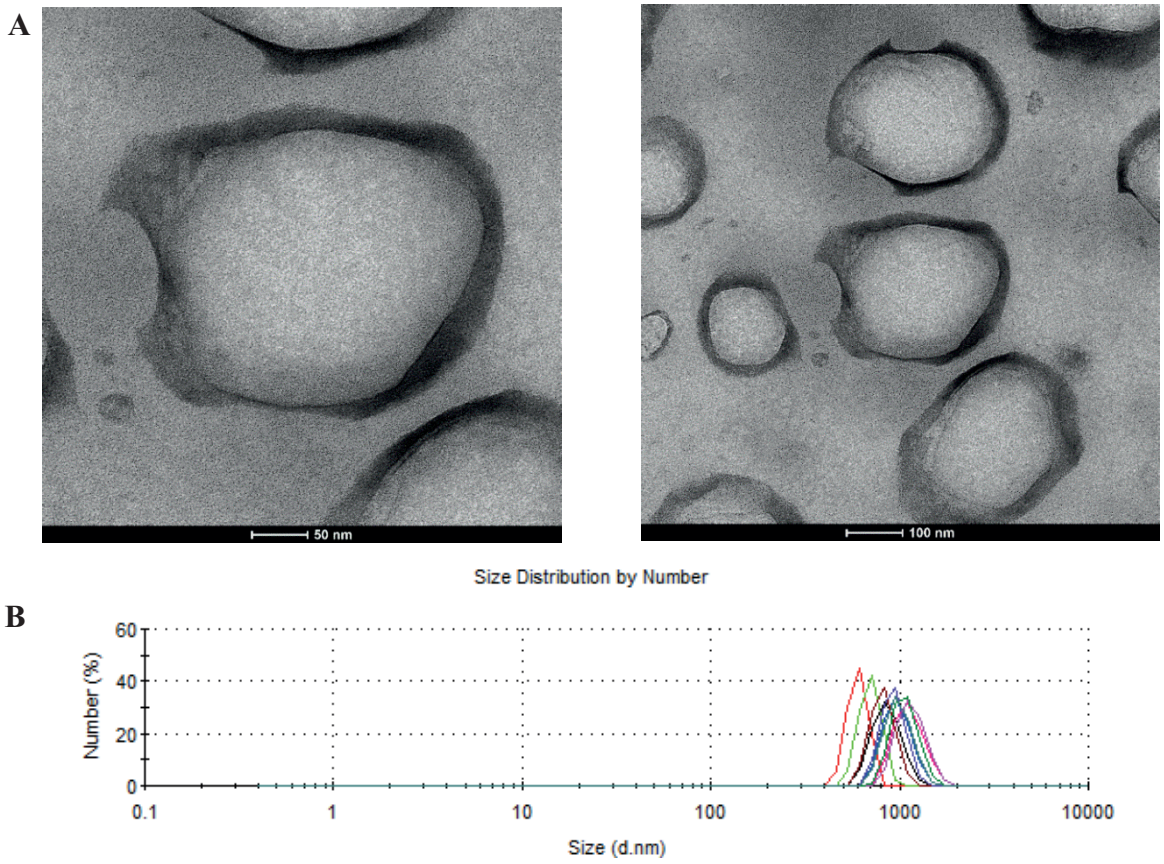

Figure 5. A. TEM images of micellar peptides after irradiation. B. Particle size distribution graph of peptide after irradiation measured by DLS.

3. Experimental

3.1. Anthraquinone-2-carboxylic acid (2)[21]

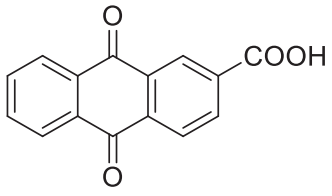

2

2-Methylanthraquinone (**1**) (1 g, 4.5 mmol) and acetic acid (50 mL) were added to a double-necked flask fitted with a condenser. A mechanical stirrer and a thermocouple were also placed into the flask. The reaction mixture was warmed gently with stirring to dissolve 2-methylanthraquinone. Then anhydrous CrO_3 (5.4 g, 54 mmol) was added slowly with vigorous stirring. The solution mixture was heated to 85 °C and kept at that temperature overnight (16 h) with stirring. Then the completed reaction mixture was cooled at room temperature and diluted with 150 mL of distilled water. The resulting precipitate was filtered and washed with water until the blue color of chromium salts disappeared. The obtained solid was recrystallized in acetic acid to yield anthraquinone-2-carboxylic acid (2) as white crystalline solid. Yield: 85%. ^{1}H NMR (400 MHz, DMSO-d_6) δ 13.73 (s, 1H), 8.64 (d, J = 1.7 Hz, 1H), 8.38 (dd, J = 8.0, 1.6 Hz, 1H), 8.28 (dd, J = 8.0, 1.9 Hz, 1H), 8.21 (dd, J = 5.1, 2.2 Hz, 2H), 8.01–7.90 (m, 2H). ^{13}C NMR (100 MHz, d_6-DMSO) δ 181.9, 181.8, 165.9, 135.6, 135.5, 134.7, 134.7, 134.4, 133.1, 133.0 (2C), 127.3, 127.2, 126.8 (2C).

3.2. Anthracene-2-carboxylic acid (3)[21]

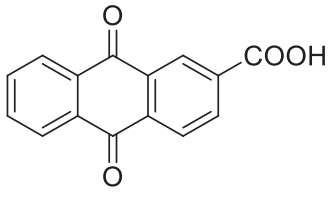

2

Anthraquinone-2-carboxylic acid (**2**) (0.5 g, 2 mmol), zinc dust (2.6 g, 40 mmol), $CuSO_4.5H_2O$ (0.1 g, 0.4 mmol), and aqueous ammonia (35 mL, 26%) were added to a 100-mL flask. The reaction mixture was stirred with a magnetic stirrer under reflux at 70 °C for 5.5 h. Then the reaction temperature was increased to 85 °C and kept for 2 h at this temperature. The completed hot reaction mixture was filtered to remove insoluble residues and the filtrate was cooled. After that, the filtrate was acidified with dilute HCl (1:1) until pH was between 4 and 5. The precipitated yellow solid was filtered and dried in a freeze dryer. Then the yellow solid was recrystallized in acetic acid. The reaction was completed with 72% yield. ^{1}H NMR (400 MHz, DMSO-d_6) δ 8.76 (s, 2H), 8.62 (s, 1H), 8.30–7.92 (m, 4H), 7.66-7.50 (m, 2H). ^{13}C NMR (100 MHz, DMSO-d_6) δ 167.4, 132.5, 132.1, 131.6, 131.5, 130.0, 128.5, 128.5, 128.3, 128.1, 127.5, 127.5, 126.7, 126.0, 124.1.

3.3. Synthesis of Ant-PK peptide

Ant-PK peptide was synthesized using standard SPPS methods on Rink amide MBHA resin (0.25 mM scale, 1.0 mmol/g loading) using a CEM Discover Bio-Manual Microwave Peptide Synthesizer (Matthews, NC, USA).

Each amino acid (3 equiv.) was coupled by HBTU (2.85 equiv.) and DIEA (6 equiv.) in DMF. A standard coupling program (20 W, 75 °C, 10 min) was used for all amino acids except for the coupling of Fmoc-Pro-OH, which were double-coupled (20 W, 75 °C, 15 min). Deprotection steps were performed in 20% piperidine in DMF (20 W, 75 °C, and 3 min) and repeated twice. Each coupling and deprotection was monitored by Kaiser test, except Fmoc-Pro-OH. The N-terminus of the peptides was extended with 6-aminohexanoic acid. After removal of final Fmoc group from N-terminal Fmoc-peptide-resin, 3.0 equivalents of anthracene-2-carboxylic acid (**3**) was coupled to the peptidyl resin with 3.3 equivalents of DIC and 3.6 equivalents of HOBt for 90 min to 2 h, at room temperature in DMF. Following the anthracene coupling, deprotection of the side chains and cleavage of the peptide from resin were done with TFA/TIS/H_2O=90:5:5 (v/v/v) for 90 min. Peptide solution was precipitated in cold ether and collected by centrifugation. The resulting peptide was lyophilized and purified using semipreparative RP-HPLC. Purity was checked with analytical RP-HPLC (Figure 6) and identity was verified by mass spectrometry (Figure 7). An Ant-PK peptide was obtained with 99.8% purity according to absorption peak at 214 nm. The mass of the purified peptide was confirmed with HRMS in positive ion mode. $[M+H]^+_{cal:}$ 1010.6191 and $[M+H]^+_{obs}$: 1010.6215.

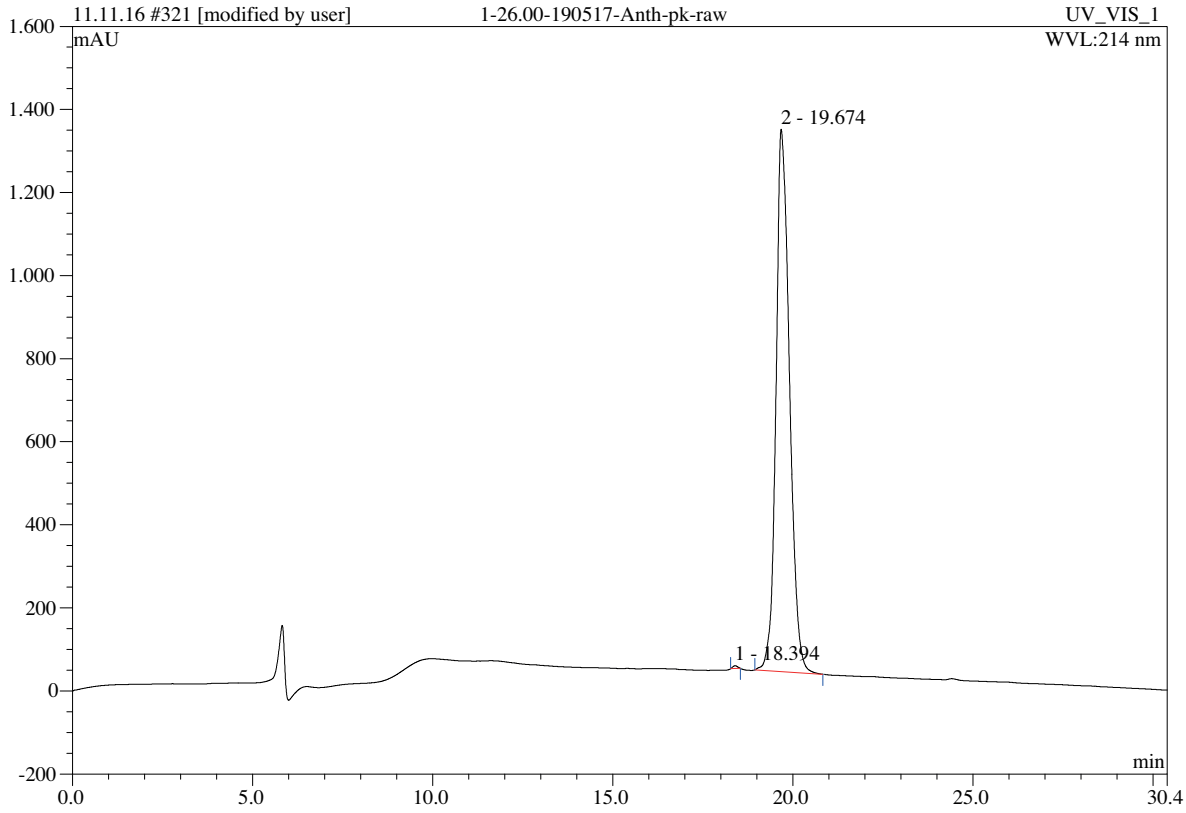

Figure 6. HPLC chromatogram of Ant-PK peptide at 214 nm.

3.4. RP-HPLC analysis

RP-HPLC was performed on a Dionex UltiMate 3000 HPLC system, employing a Thermo Scientific Hypersil Gold C18 column (250 × 10 mm, 5 μm) (Waltham, MA, USA) at a flow rate of 2 mL/min at 40 °C.

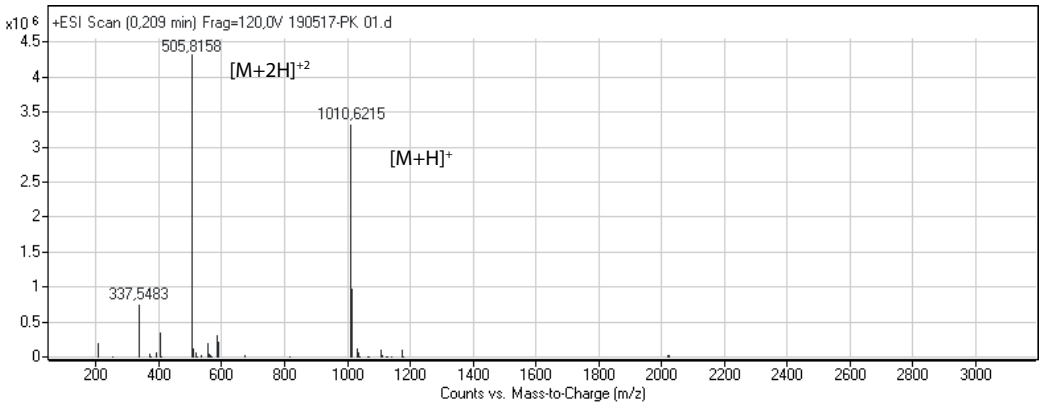

Figure 7. High-resolution mass spectrum of Ant-PK peptide.

Acetonitrile/water gradient containing 0.1% trifluoroacetic acid (5%–100%, 1–70 min) was utilized as eluent. Peptide was dissolved in 10% acetic acid solution. The concentration of the peptide was adjusted to 20 mg/mL. Of this peptide solution, 1.5 mL was purified for one batch by 2-mL injection loop and purification repeated consecutively. The purity of each fraction was assessed with analytical RP-HPLC before combining pure fractions.

Analytical HPLC was performed on a Dionex UltiMate 3000 HPLC system (Sunnyvale, CA, USA) equipped with a Thermo Scientific Acclaim 120 C18 column (46 × 150 mm, 3 μm). Elution of the peptides was achieved using an acetonitrile/water gradient containing 0.1% trifluoroacetic acid (5%–100%, 1–30 min, flow 0.4 mL/min). After purity of collected fractions confirmed by analytical HPLC, lyophilization was achieved using a Telstar Cryodos Freeze Dryer (Bristol, PA, USA) and peptide was stored at –20 °C.

3.5. Mass analysis of peptide

The concentration of synthesized peptide was adjusted to 1 mg/mL with water and characterized by mass spectrometry on an Agilent 6530 Q-TOF mass spectrometer equipped with an electrospray ionization source (Santa Clara, CA, USA).

3.6. NMR analysis

^{1}H NMR and ^{13}C NMR spectra were recorded on a Bruker 400 MHz spectrometer (Billerica, MA, USA) with DMSO-d_6 as a solvent. Unless otherwise indicated, chemical shifts are reported in ppm downfield from tetramethylsilane at room temperature using deuterated solvents as an internal standard. Abbreviations used for splitting patterns are as follows: s = singlet, br s = broad singlet, d = doublet, t = triplet, and m = multiplet.

3.7. TEM

TEM measurements were performed on a JEM-2100F (JEOL, Tokyo, Japan) microscope operating at 200 kV. Aliquots of 0.5 mM peptide solutions were gently dripped onto holey carbon coated TEM grids and the grids were negatively stained with 1 wt. % aqueous uranyl acetate solution in water; excess materials were removed by washing with water. TEM samples were air-dried for 3 h prior to imaging.

3.8. DLS measurements

Before and after irradiation, hydrodynamic sizes of micellar Ant-PK peptides were measured using a Zetasizer Nano-ZS (Malvern Instruments Ltd., Malvern, UK). Average hydrodynamic sizes were obtained by cumulative analysis of autocorrelation data. Samples were placed in polystyrene cells, which were cleaned with ultrapure water. Measurements were taken 10 times at 25 °C in order to check their reproducibility.

3.9. Photodimerization reaction

Samples were irradiated with a mercury medium pressure lamp. The lamp is contained in double-walled immersion wells made of quartz, allowing water cooling and/or filtering of excitation radiation. All irradiations were carried out for 10 min and repeated three times.

3.10. Fluorescence spectroscopy

Fluorescence spectra were recorded on a Varian Cary Eclipse fluorescence spectrophotometer (Agilent). All spectra were taken at room temperature with an integration time of 0.1 s. The slit width was set at 5 nm for excitation and emission. Emission spectra were obtained from 380 to 600 nm with excitation at 365 nm. The EMT detector voltage was arranged at 480 nm.

Acknowledgments

Financial support provided by METU-BAP, OYP program, and TÜBİTAK BİDEB 2211/A scholarship is gratefully acknowledged. For instrumental usage, we also would like to thank Prof Dr Ahmet Önal (fluorescence spectrometry), Dr İrem Erel Göktepe (DLS), and Dr Yunus Emre Türkmen (photoreactor).

References

1. Mura, S.; Nicolas, J.; Couvreur, P. *Nat. Mater.* **2013**, *12*, 991-1003.
2. Ding, C.; Tong, L.; Feng, J.; Fu, J. *Molecule*s **2016**, *21*, 1715-1745.
3. Aznar, E.; Oroval, M.; Pascual, L.; Murguía, J. R.; Martínez-Máñez, R.; Sancenón, F. *Chem. Rev.* **2016**, *116*, 561-718.
4. Mal, N. K.; Fujiwara, M.; Tanaka, Y. *Nature* **2003**, *421*, 350-353.
5. Mal, N. K.; Fujiwara, M.; Tanaka, Y.; Taguchi, T.; Matsukata, M. *Chem. Mater.* **2003**, *15*, 3385-3394.
6. Kihara, H.; Yoshida, M. *ACS Appl. Mater. Interfaces* **2013**, *5*, 2650-2657.
7. Wang, C.; Zhang, D.; Xiang, J.; Zhu, D. *Langmuir* **2007**, *23*, 9195-9200.
8. Al-Kaysi, R.; Bardeen, C. *Adv. Mater.* **2007**, *19*, 1276-1280.
9. Ikegami, M.; Ohshiro, I.; Arai, T. *Chem. Commun.* **2003**, *13*, 1566-1567.
10. Liu, Y.; Chang, H.; Jiang, J.; Yan, X.; Liu, Z.; Liu, Z. *RSC Adv.* **2014**, *4*, 25912-25915.
11. Jezowski, S. R.; Zhu, L.; Wang, Y.; Rice, A. P.; Scott, G. W.; Bardeen, C. J.; Chronister, E. L. *J. Am. Chem. Soc.* **2012**, *134*, 7459-7466.
12. Chen, W.; Wang, J.; Zhao, W.; Li, L.; Wei, X.; Balazs, A. C.; Russell, T. P. *J. Am. Chem. Soc.* **2011**, *133*, 17217-17224.
13. Becker, H. D. *Chem. Rev.* **1993**, *93*, 145-172.
14. Xu, J.; Chen, Y.; Wu, L.; Tung, C.; Yang, Q. *Org. Lett.* **2013**, *15*, 6148-6151.

15. Good, J. T.; Burdett, J. J.; Bardeen, C. J. *Small* **2009**, *5*, 2902-2909.

16. Islangulov, R. R.; Castellano, F. N. *Angew. Chem. Int. Ed.* **2006**, *45*, 5957-5959.

17. Dvornikov, A. S.; Bouas-Laurent, H.; Desvergne, J.; Rentzepis, P. M. *J. Mater. Chem.* **1999**, *9*, 1081-1084.

18. Shi, Y.; Cardoso, R. M.; van Nostrum, C. F.; Hennink, W. E. *Polym. Chem.* **2015**, 6, 2048-2053.

19. Wells, L. A.; Brook, M. A.; Sheardown, H. *Macromol. Biosci.* **2011**, 11, 988-998.

20. Wells, L. A.; Furukawa, S.; Sheardown, H. *Biomacromolecules* **2011**, 12, 923-932.

21. Arjunan, P.; Berlin, K. D. *Org. Prep. Proced. Int.* **1981**, *13*, 368-371.

22. Guler, M. O.; Claussen, R. C.; Stupp, S. I. *J. Mater. Chem.* **2005**, *15*, 4507-4512.